Expression of VEGF, semaphorin SEMA3F, and their common receptors neuropilins NP1 and NP2 in preinvasive bronchial lesions, lung tumours, and cell lines.

Sylvie Lantuejoul, Bruno Constantin, Harry A. Drabkin, Christian Brambilla, Joëlle Roche, Elisabeth Brambilla

Journal of Pathology
J Pathol 2003; **200**: 336–347.
Published online 20 March 2003 in Wiley InterScience (www.interscience.wiley.com). **DOI:** 10.1002/path.1367

Original Paper

Expression of VEGF, semaphorin SEMA3F, and their common receptors neuropilins NP1 and NP2 in preinvasive bronchial lesions, lung tumours, and cell lines

Sylvie Lantuéjoul,[1] Bruno Constantin,[3] Harry Drabkin,[4] Christian Brambilla,[1] Joëlle Roche[2] and Elisabeth Brambilla[1]*

[1]*Laboratoire de Pathologie Cellulaire, INSERM U 578, Grenoble, France*
[2]*IBMIG, FRE CNRS 2224, Université de Poitiers, Poitiers, France*
[3]*LBSC, UMR CNRS 6558, Université de Poitiers, Poitiers, France*
[4]*University of Colorado Health Sciences Center, Division of Medical Oncology, Denver, CO, USA*

**Correspondence to: Professor Elisabeth Brambilla, Service de Pathologie Cellulaire, CHU Albert Michallon BP 217, 38043 Grenoble Cedex 09, France.*
E-mail: EBrambilla@chu-grenoble.fr

Received: 18 July 2002
Revised: 6 November 2002
Accepted: 28 January 2003

Abstract

Two receptors, neuropilin 1 (NP1) and neuropilin 2 (NP2), bind class 3 semaphorins, axon guidance molecules including SEMA3F, the gene for which was isolated from a 3p21.3 deletion in lung cancer. In addition, they bind VEGF (vascular endothelial growth factor), enhancing the effects of VEGF binding to KDR/Flk-1. Elevated VEGF levels are associated with the loss and cytoplasmic delocalization of SEMA3F in lung cancer, suggesting competition for their NP1 and NP2 receptors. To determine the timing of these events, we compared by immunohistochemistry VEGF, SEMA3F, NP1 and NP2 expression in 50 preneoplastic lesions and 112 lung tumours. In preneoplastic lesions, VEGF increased from low-grade to high-grade dysplasia ($p = 0.001$) whereas SEMA3F levels remained low. NP1 and NP2 levels increased from dysplasia to microinvasive carcinoma ($p = 0.0001$) and correlated with VEGF expression ($p = 0.04$ and 0.0002, respectively). Non-small cell lung carcinoma overexpressed VEGF and NP1 and NP2 significantly more often than neuroendocrine tumours including small cell lung carcinoma. SEMA3F loss or delocalization correlated with advanced tumour stage. Migrating cells overexpressed VEGF, SEMA3F, NP1 and NP2 with cytoplasmic delocalization of NP1 as demonstrated in an *in vitro* wound assay. These results demonstrate early alteration of the VEGF/SEMA3F/NP pathway in lung cancer progression. Copyright © 2003 John Wiley & Sons, Ltd.

Keywords: semaphorin (SEMA3F); neuropilins; VEGF; preneoplastic bronchial lesions; lung tumours

Introduction

Lung cancer is the leading cause of cancer-related deaths in industrial countries, cigarette smoking being the main risk factor, responsible for 90% and 78% of lung carcinoma in men and women, respectively. Most patients present with advanced disease and a poor prognosis despite improvements in clinical treatments [1]. Understanding the molecular pathogenesis of lung cancer may help to provide new and more sensitive means for early detection of lung cancer and for its therapy [2]. According to the WHO histological classification [3], the major classes of lung tumour comprise squamous cell carcinoma (SCC), small cell lung carcinoma (SCLC), adenocarcinoma (ADC), large cell carcinoma, including two recently described variants — large cell neuroendocrine carcinoma (LCNEC) and basaloid carcinoma (BC) — and typical and atypical carcinoid tumours.

Preneoplastic lesions accompanying and preceding SCC and BC are suspected to develop in conjunction with a multistep accumulation of genetic alterations that progressively transforms normal bronchial epithelium to invasive carcinoma [4]. Morphologically, lesions progress from hyperplasia to squamous metaplasia, dysplasia of various degrees (mild, moderate and severe) and then *in situ* and invasive carcinoma. Whether hyperplasia and squamous metaplasia represent common reactive changes or true neoplasia is not certain; they are thus considered along with mild dysplasia as low-grade preneoplastic lesions. In contrast, moderate and severe dysplasia and *in situ* carcinoma are high-grade premalignant lesions [2,5]. To understand these lesions better from a molecular standpoint, and to provide specific intermediate endpoints for chemopreventive studies, new biomarkers are needed to define the stepwise process of lung cancer development and the chronology by which genetic and epigenetic changes develop [6–8].

VEGF, one of the key factors in tumour angiogenesis [9], is upregulated in numerous benign and malignant tumours. The biological effects of $VEGF_{165}$ are mediated by two tyrosine kinase receptors: VEGF-R1 (Flt-1) and VEGF-R2 (KDR/Flk-1). The prevailing

concept has been that VEGF is secreted by tumour cells and its receptors are expressed by endothelial cells, enhancing their proliferation and migration in a paracrine manner. VEGF has been substantially implicated in tumour development since VEGF inhibition suppresses tumour growth *in vivo*, limiting neovascularization [10]. Moreover, the demonstration of increased vessel density related to VEGF secretion in preneoplastic bronchial lesions [11] implicates VEGF and its receptors in early lung cancer progression. However, one preneoplastic lesion observed exclusively in smokers — angiogenic squamous dysplasia, described by Keith *et al* [12] as micropapillary angiogenic lesions — was not clearly associated with a greater risk for cancer progression, although VEGF expression was suspected to be higher than in ordinary dysplastic lesions occurring in smokers. Thus, the role or timing of VEGF expression in premalignant lesions still needs to be defined more precisely.

Two other transmembrane VEGF receptors, NP1 and NP2 [13,14], were initially identified in neuronal cells as receptors for class 3 semaphorins (see semaphorin nomenclature 1999) [15]. NP1 is expressed by endothelial cells and corresponds to a VEGF co-receptor enhancing VEGFR2/KDR binding [16], tumour angiogenesis and progression [17]. NP1 expression was also reported in adult tissues, exhibiting high levels in heart and placenta, moderate levels in lung, liver, and kidney, and low levels in brain. NP1 expression was also identified in tumour-derived cells such as those from breast and prostate carcinoma [16], suggesting that VEGF might be involved in an autocrine loop through its neuropilin receptors. The previous view that VEGF-R1 and R2 were not expressed on tumour cells has been recently revised. Several tumour cells also express VEGF-R1 or VEGF-R2, including lung cancer cells [18,19], confirming that tumour cells participate in a functional autocrine loop via several receptors. NP2, which shares 47% homology with NP1, is absent from endothelial cells but is expressed in mouse embryonic lung [20] and in tumours including osteosarcoma, where its expression correlates with a poor prognosis [21], as well as in melanoma, where NP1, NP2, and KDR have been implicated in a proliferative response [22].

The other ligands of neuropilins are class 3 semaphorins [15]. The widespread expression of semaphorins suggested that they had other functions outside the nervous system: this was subsequently demonstrated in normal lung development [23] and in tumorigenesis [24,25]. As SEMA3F was previously isolated in SCLC cell lines from a recurring homozygous deletion at 3p21.3, a region that also undergoes LOH in tumours, it has been suggested that this gene is a tumour suppressor gene [26,27]. While SEMA3A binds only NP1 [13,14], SEMA3F binds both NP1 and NP2 [28,29] with 10 times more affinity for NP2, and thus shares these receptors with $VEGF_{165}$ in endothelial and tumour cells. Competition between SEMA3A and $VEGF_{165}$ has been demonstrated [30,31] and a balance between these two molecules mediates migration and apoptosis of neural progenitors [32]. Furthermore, we found that in lung tumours high VEGF expression was associated with decreased levels of SEMA3F membrane staining and cytoplasmic delocalization [25]. This suggested that SEMA3F and VEGF might compete for binding to their common receptors and that loss of SEMA3F would confer a growth advantage to tumours. In the present study, we screened 50 preneoplastic bronchial lesions associated with lung carcinomas and a larger panel of 112 lung tumours for expression of VEGF, SEMA3F, NP1, and NP2, by immunohistochemistry. In addition, we performed confocal microscopic analysis on a set of normal and tumour cell lines to characterize the localization of these proteins and to study the timing of their expression in a wound assay.

Material and methods

Cell lines

The lung cell lines studied included NHBE (normal human bronchial epithelial cells), BAES2B (SV40-immortalized bronchial epithelium) and NCI-H661 (non-small cell lung carcinoma cells) and they were compared with HUVEC (human umbilical vein endothelial cells) and HeLa cells (cervical adenocarcinoma cells). NHBE and HUVEC were obtained from Clonetics and grown in BEGM bullekit media and EGM bullekit media respectively. BAES2B, NCI-H661 and HeLa were obtained from ATCC and were grown in RPMI-1640 containing 10% fetal calf serum under 5% CO_2.

Tumour tissue samples

One hundred and twelve primary lung tumours were retrieved from the frozen bank of the Cellular Pathology Department. Local ethical guidelines were followed. Tumours were classified according to the 1999 World Health Organization (WHO) histological classification of lung tumours as follows: 42 squamous cell carcinoma (SCC), 9 small cell lung carcinoma (SCLC), 34 adenocarcinoma (ADC), 12 large cell neuroendocrine carcinoma (LCNEC), 4 basaloid carcinoma, and 7 typical and 4 atypical carcinoids (TC and AC respectively). Fifty preneoplastic bronchial lesions from 25 patients with associated invasive carcinoma, where preinvasive lesions were identified on frozen examination of the resection margins, were studied immunohistochemically, including 10 mild dysplasia, 14 moderate dysplasia, 12 severe dysplasia and 14 carcinoma *in situ* (CIS). Among these, 17 disclosed an angiogenic papillary pattern according to the description of Keith *et al* [12] (one mild dysplasia, 4 moderate dysplasia, 6 severe dysplasia and 6 CIS). These preneoplastic lesions were compared with 19 hyperplastic bronchial mucosae and

10 squamous bronchial metaplasia identified in the same resected lung tumours including 16 SCC (12 invasive and 4 microinvasive), 4 basaloid carcinoma (BC), 3 ADC, and 2 LCNEC. Tumour samples were obtained from these surgical lung resections or from mediastinal lymph node biopsies performed during mediastinoscopy in non-operable patients as a diagnostic procedure. One of the tumour samples was quickly frozen before histological sampling. For clinicopathological correlation, TNM disease stages were evaluated according to the international UICC classification. Eighteen of 42 SCC, 1 of 4 BC, 6 of 34 ADC, 1 of 11 carcinoid tumours, 6 of 12 LCNEC, and all SCLC patients presented at advanced tumour stage (III–IV).

Immunohistochemical analysis of tissue samples

Immunostaining of VEGF, SEMA3F, NP1, and NP2 was performed on frozen sections. The primary rabbit polyclonal antibodies used were anti-VEGF A20 (Santa Cruz Biotechnology, Santa Cruz, USA) at a dilution of 1 : 800, anti- SEMA3F, previously described [33] and used at a dilution of 1 : 50, anti-NP1 (Santa Cruz Biotechnology, Santa Cruz, USA) at a dilution of 1 : 100, and anti- NP2 (Santa Cruz Biotechnology, Santa Cruz, USA) at a dilution of 1 : 100. After fixation in cold acetone for 10 min and blocking of non-specific binding with 2% donkey serum for 30 min, a three-stage indirect immunoperoxidase technique was used: incubation with the primary antibody at 4 °C overnight, followed by the secondary biotinylated donkey anti-rabbit immunoglobulin G (Jackson, Baltimore, PA) (1 : 1250) then the amplification system avidin–biotin complex (Dakopatts, Glostrup, Denmark) (1 : 200). Negative control consisted of omission of the primary antibody and incubation with immunoglobulin of the same species at the same final concentration. To assess the specificity of VEGF and SEMA3F antibodies, *in vitro* immunoneutralization was performed by preincubating the primary antibody with a 10 times excess weight of immunizing peptides (VEGF A20 blocking peptide, Santa Cruz, and the 16-amino acid SEMA3F peptide) for 2 h at room temperature in order to abolish the immunostaining. No blocking peptides were available for NP1 and NP2 *in vitro* immunoneutralization, but these antibodies (from Santa Cruz) gave immunostaining results with 85% concordance (intensity and percentage of labelled cells) with NP1 and NP2 antibodies kindly provided by A. Kolodkin on 104 lesions from these series stained concomitantly with the two NP1 and NP2 antibodies. Staining scores were established by semi-quantitative optical analysis, using the product of percentage of positive cells and staining intensity from 1 to 3 (1 weak, 2 moderate, and 3 strong), and therefore ranged from 0 to 300. Cases with a score greater than 10 were considered to be positive.

Immunostaining and confocal microscopy on cell lines

For NP1 and NP2 immunostaining, cell fixation was performed in 1% paraformaldehyde for 15 min with saponin 0.1% permeabilization for 10 min. Anti-NP1 rabbit polyclonal antibody (gift from Dr A. L. Kolodkin, Baltimore) raised against amino acids 583–856 of rat NP1 [13] was used at a dilution of 1 : 1000. Anti-NP2 polyclonal antibody (Santa Cruz Biotechnology, Santa Cruz, USA) was used at a dilution of 1 : 100. Immunostaining for SEMA3F was performed as described previously [25]. Cells were exposed in the dark to a second RRX-conjugated goat anti-rabbit antibody diluted at 1 : 200 (Jackson Immunoresearch Lab, Inc.) and mounted using Vectashield (Vector, Burlingame, CA, USA). Immunostained samples were examined using the yellow line (568 nm) of the confocal microscope (BioRad MRC, Hemel Hempstead, UK) equipped with a 15 mW argon–krypton gas laser.

Quantitative RT-PCR

In order to confirm the presence of transcripts sustaining expression of the proteins detected immunohistochemically, and to justify the validity of the antibodies, we investigated the presence of VEGF, SEMA3F, NP1, and NP2 mRNA in addition to protein expression in 11 lung tumours (6 SCC and 5 ADC) and two cell lines using real-time RT-PCR, where protein expression was immunohistochemically assessed. The frozen material used for mRNA extraction was analysed morphologically on a frozen section in order to assess the proportion of stromal cells. The cases chosen for this comparison (mRNA–protein) contained more than 60% tumour cells (less than 40% stromal cells). It would not have been accurate to compare expression in tumours to normal lung, as the latter is a highly vascularized tissue where endothelial cells are the predominant cell type. Therefore, an immortalized cell culture derived from lung epithelium, NHBE, was used as normal lung epithelium. Conversely, NCI-H661, which failed to exhibit positive immunocytochemical staining with NP1 and NP2 antibodies, was studied to estimate NP1 and NP2 transcripts.

Total RNA and cDNA were prepared as described previously [25]. We assessed levels of SEMA3F, NP1, NP2, and VEGF transcription relative to G3PDH in lung tumours by quantitative real-time RT-PCR carried out using the GeneAmp 5700 (ABI) system with SYBR Green chemistry as described previously [25]. PCR was carried out in 50 µl reaction volumes consisting of 1 × PCR SYBR Green buffer, 0.25 µM primers, 200 µM dNTPs, and 0.03 units/µl AmpliTaq Gold (Perkin-Elmer). cDNA was amplified as follows: 50 °C for 2 min, 95 °C for 10 min, followed by 40 cycles at 95 °C × 15 s, 60 °C × 1 min. SEMA3F, NP1, NP2, and VEGF cDNA were amplified with the following primers: SEMA3F forward

5′AGCAGACCCAGGACGTGAG3′ and SEMA3F reverse 5′AAGACCATGCGAATATCAGCC3′ giving a 112 bp product; $VEGF_{165}$ forward 5′CAAGACAAGAAAATCCCTGTGG3′ and $VEGF_{165}$ reverse 5′CCTCGGCTTGTCACATCTG3′ giving a 162 bp product; NP2 forward 5′GGATGGCATTCCACATGTTG3′ and NP2 reverse 5′ACCAGGTAGTAACGCGCAGAG3′ giving a 152 bp product; NP1 forward 5′ATCACGTGCAGCTCAAGTGG3′ and NP1 reverse 5′TCATGCAGTGGGCAGAGTTC3′ giving a 167 bp product. The raw data were obtained in terms of Ct values, which refers to the PCR cycle number during exponential amplification at which the product (measured in real time by SYBR Green fluorescence) crosses an arbitrary threshold. To adjust for variations in the amount of RNA, the Ct values for each gene were normalized against the Ct values for the housekeeping gene G3PDH (ie delta $Ct = Ct_{\text{specific gene}} - Ct_{\text{G3PDH}}$). While the resulting delta Ct values are experimentally convenient, they are not readily intuitive (ie they reflect exponential amplification and higher delta Cts represent lower expression). Instead, the results are displayed in terms of the relative expression ($\times 1000$) compared to G3PDH. For instance, a value of 1000 is equal to the expression of G3PDH and a value of 100 is equivalent to 10% of the G3PDH level.

Statistical analysis

The staining scores were compared in different categories using the Mann–Whitney U-test, Kruskal–Wallis H and Spearman tests. All the tests were performed with the Stat View programme (Abacus Concepts, Berkeley, CA).

Results

Immunohistochemical analysis of VEGF in normal lung, preinvasive bronchial lesions, and corresponding invasive carcinomas (Table 1)

VEGF was highly expressed in normal lung by bronchial basal cells (Figure 1A), as well as by hyperplastic type II pneumonocytes (scores = 100–200). Cytoplasmic staining was associated with stronger membrane staining at the apical surface. Endothelial cells and smooth muscle cells were also stained, but with lower scores not exceeding 50.

In preinvasive and invasive bronchial lesions, epithelial cells, endothelial cells, and stromal fibroblasts exhibited strong VEGF cytoplasmic staining, often with membrane accentuation (Figure 1B, J). VEGF expression increased significantly with the severity of histological grade in preneoplastic lesions ($p = 0.0001$). Scores were significantly lower in hyperplastic mucosa than in squamous metaplasia and mild dysplasia ($p = 0.0017$), and lower in low-grade preneoplastic lesions (squamous metaplasia and mild dysplasia) than in high-grade lesions (moderate, severe dysplasia and CIS) ($p = 0.0001$). VEGF scores were also higher in severe dysplasia and CIS than in microinvasive and corresponding invasive carcinomas, SCC and BC ($p = 0.014$). Moreover, high VEGF expression was observed in discrete clusters of dysplastic cells of low-grade preneoplastic lesions, and became homogeneous and more intense in corresponding high-grade lesion from the same patient. Overall, increasing levels of VEGF expression were observed during the process of preneoplastic transformation that culminated in invasive carcinoma.

No difference could be detected between VEGF expression in angiogenic papillary preneoplastic lesions (angiogenic squamous dysplasia) and that of classical dysplastic lesions of similar histological grade.

Immunohistochemical analysis of SEMA3F in normal lung, preinvasive lesions, and corresponding carcinomas (Table 1)

SEMA3F was expressed on alveolar type II pneumonocytes with a membrane pattern (score = 300) and on bronchial basal and bronchiolar cells with a cytoplasmic and membrane pattern (score = 100) (Figure 1C). Endothelial cells of alveolar capillaries remained negative, whereas those of arterioles and venules displayed mild cytoplasmic staining without membrane staining. In preinvasive and invasive bronchial lesions, SEMA3F staining

Table 1. Immunostaining scores for VEGF, SEMA 3F, NP1, and NP2 in preneoplastic bronchial lesions and corresponding SCC and BC (mean scores ± SD)

Histology	N	VEGF mean scores ± SD	SEMA3F mean scores ± SD	NP1 mean scores ± SD	NP2 mean scores ± SD
Hyperplastic mucosae	19	17 ± 36	27 ± 59	76 ± 31	72 ± 26
Squamous metaplasia	10	47 ± 53	1 ± 2	131 ± 78	117 ± 71
Mild dysplasia	10	25 ± 13	37 ± 76	152 ± 71	140 ± 71
Moderate dysplasia	14	92 ± 62	40 ± 50	169 ± 53	174 ± 49
Severe dysplasia	12	172 ± 84	61 ± 69	175 ± 80	186 ± 53
In situ carcinoma	14	166 ± 81	68 ± 77	166 ± 69	169 ± 58
Microinvasive carcinoma	4	103 ± 54	69 ± 90	200 ± 61	188 ± 73
Corresponding SCC and BC	16	111 ± 65	70 ± 71	84 ± 53	99 ± 57

SCC, squamous cell carcinoma; BC, basaloid carcinoma.

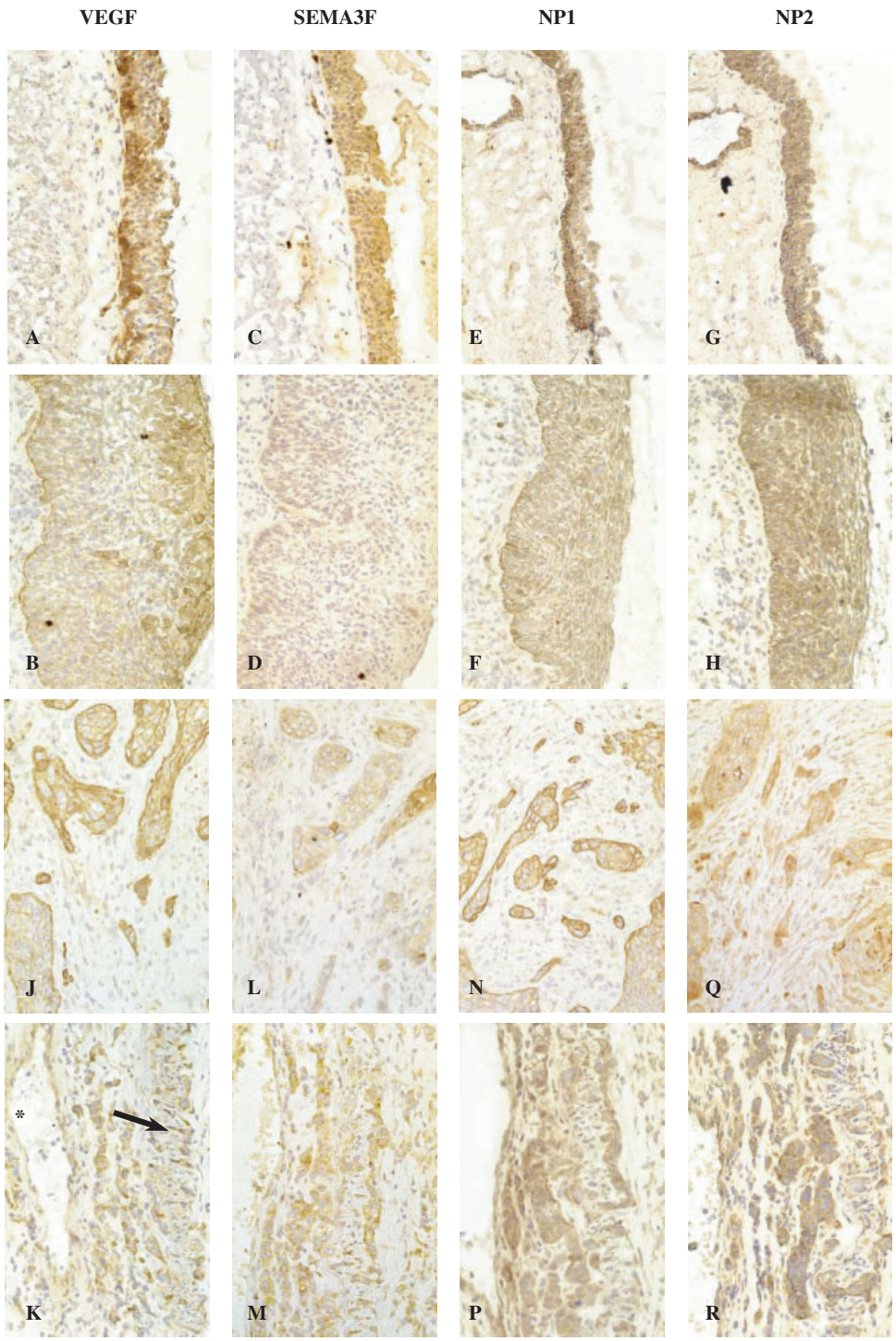

Figure 1. Immunohistochemical staining of normal bronchial epithelium, preneoplastic lesions and in corresponding lung tumours (immunoperoxidase staining). *Normal bronchial epithelium and preneoplastic lesions* (A–H): (A,B) VEGF immunostaining is restricted to the basal layer in normal bronchioles (A). It is strongly expressed and extends throughout the full thickness of the epithelium in this severe dysplasia (B). (C, D) Semaphorin 3F immunostaining is moderate in normal bronchial epithelium (C) and faint in this severe dysplasia (D). (E,F) NP1 immunostaining on bronchial cells with membrane accentuation on basal cells (E). Strong NP1 expression is shown in this severe dysplasia, with a membrane pattern of staining (F). (G,H) NP2 immunostaining with moderate intensity on normal bronchial cells (G). This staining is expended to the full thickness in severe dysplasia (H). *Migration and invasion in corresponding lung tumours* (J–R): (J, K) Strong cytoplasmic and membrane VEGF staining in a squamous cell carcinoma (SCC) with small clusters of cells isolated in the stroma, infiltrating away from the tumour bulk on serial sections (J) and, in an adenocarcinoma (ADC), cells in trabeculae invading an arterial vessel wall (*lumen, → muscular media) (K). (L, M). Moderate SEMA3F cytoplasmic staining in the same lesions as J and K (SCC: L and ADC: M). (N, P) Strong NP1 cytoplasmic staining with membrane accentuation in the same lesions as J and K (SCC: N and ADC: P). (Q, R) Strong cytoplasmic NP2 staining in the same lesions as J and K (SCC: Q and ADC: R, with membrane staining)

varied from either cytoplasmic to cytoplasmic and membranous (Figures 1D, L). Weak SEMA3F staining was observed in hyperplastic mucosa and squamous metaplasia, while mean scores were slightly higher in dysplasia, CIS, and in corresponding microinvasive and invasive SCC and BC. However, no statistical differences were observed between different histological grades whether considered individually, or when low-grade and high-grade preneoplastic lesions were compared. This mild increase in scores was considered to be the result of a higher number of positive cells consistent with polystratification of positive basal cells and increased thickness of the epithelium, but was not due to increased staining intensity of individual cells. In contrast with low-grade preneoplastic lesions, SEMA3F expression was predominantly cytoplasmic in high-grade preneoplastic lesions and their invasive counterparts. These results indicate that reduced SEMA3F staining and cytoplasmic delocalization occur early in lung cancer pathogenesis.

Immunohistochemical analysis of NP1 and NP2 in normal lung, preinvasive lesions, and corresponding carcinomas (Table 1)

In normal lung, NP1 and NP2 expression was detected exclusively in bronchial basal cells of normal epithelium with a cytoplasmic and membrane pattern, and in smooth muscle cells with a cytoplasmic pattern (scores = 200–300) (Figure 1E, G). In preinvasive and invasive bronchial lesions, NP1 and NP2 staining was cytoplasmic in epithelial cells with strong membrane accentuation (Figure 1F, H, N, Q). Endothelial cells stained strongly with the NP1 antibody and weakly with the NP2 antibody.

The mean NP1 and NP2 scores increased significantly from hyperplastic mucosa, squamous dysplasia, mild dysplasia, and moderate dysplasia, reaching a plateau in severe dysplasia, CIS, and microinvasive carcinoma. Severe dysplasia and CIS exhibited high scores (>120) for both NP1 and NP2. In low- and high-grade preneoplastic lesions, some clusters of dysplastic cells exhibited strong NP1 and NP2 staining. In contrast to severe dysplasia, CIS and microinvasive areas, mean scores decreased in frankly invasive areas of SCC and BC ($p = 0.0001$ for NP1 and NP2 respectively). Only 7/12 cases with anti-NP1 and 8/12 cases with anti-NP2 had scores greater than 50.

Statistical correlations between expressions of VEGF, SEMA3F, NP1, and NP2 in preinvasive bronchial lesions and invasive carcinoma

A significant correlation was observed between VEGF and NP2 expression ($p = 0.02$), and between VEGF and NP1 expression ($p = 0.05$) in hyperplasia and low-grade preneoplastic lesions. Similarly, a significant correlation was observed in high-grade preneoplastic lesions, microinvasive and corresponding invasive SCC and BC between VEGF and NP1 ($p = 0.04$) and between VEGF and NP2 ($p = 0.0002$). No correlation was found between SEMA3F and NP1 or NP2 score in preneoplastic lesions or in corresponding invasive SCC and BC. Although no significant inverse relationship was identified between VEGF and SEMA3F staining, the rank of VEGF expression was significantly higher than that of SEMA3F expression in both low-grade and high-grade preinvasive lesions ($p = 0.001$ for both; Mann–Whitney test).

VEGF, SEMA3F, NP1, and NP2 immunohistochemical expression in lung tumours (Table 2)

VEGF was expressed in most lung tumours but mean VEGF scores were significantly higher in SCC and ADC than in neuroendocrine tumours ($p = 0.0016$). The expression of VEGF was often more intense at the periphery of the tumour lobules than inside. Small clusters of cells isolated from the tumour bulk in the stroma or invading vascular structures were highly stained (Figure 1J, K). Stromal cells including endothelial cells and fibroblasts also strongly expressed VEGF in a diffuse pattern.

SEMA3F was lost in 30/80 (37%) of NSCLC, with low mean scores in SCC, LCNEC, and SCLC, in contrast to those observed in ADC and carcinoid tumours ($p = 0.0001$). Diffuse cytoplasmic staining predominated in most histological subtypes, in contrast to carcinoid tumours and bronchioloalveolar carcinoma, which exhibited membrane and cytoplasmic staining in 82% of cases. These latter tumours exhibited a unique pattern of SEMA3F/VEGF expression, with SEMA3F scores being higher than those of VEGF and with maintenance of a membrane staining pattern for SEMA3F. In other tumour types, small clusters of cells in the peritumoural stroma, which appeared to represent migrating tumour cells, exhibited strong membrane staining with SEMA3F antibody (Figures 1L, M) concomitant with VEGF expression. Stromal cells

Table 2. Immunostaining distribution and scores for VEGF, SEMA3F, NP1, and NP2 in each histological type of lung tumour (number of cases followed by % of positive cases, and mean scores ± SD)

Histology	N	VEGF	SEMA3F	NP1	NP2
SCC	42	35 (85%)	20 (48%)	27 (64%)	32 (76%)
		116 ± 64	66 ± 65	79 ± 57	87 ± 55
BC	4	2 (50%)	2 (50%)	3 (75%)	4 (100%)
		62 ± 75	7.5 ± 9	72 ± 22	107 ± 61
ADC	34	26 (76%)	28 (82%)	17 (50%)	28 (82%)
		118 ± 73	126 ± 71	60 ± 52	88 ± 47
TC + AC	11	9 (81%)	11 (100%)	6 (54%)	9 (81%)
		78 ± 69	162 ± 89	28 ± 36	46 ± 36
LCNEC	12	12 (100%)	8 (63%)	9 (73%)	11 (90%)
		82 ± 98	45 ± 54	37 ± 39	78 ± 44
SCLC	9	7 (77%)	8 (88%)	2 (22%)	6 (66%)
		41 ± 55	55 ± 53	7 ± 13	38 ± 40

SCC, squamous cell carcinoma; BC, basaloid carcinoma; ADC, adenocarcinoma; TC, typical carcinoid; AC, atypical carcinoid; LCNEC, large cell neuroendocrine carcinoma; SCLC, small cell lung carcinoma.

were negative with the exception of 20% of endothelial cells.

Both NP1 and NP2 were expressed in most SCC and ADC cases. The pattern of staining was predominantly cytoplasmic with membrane accentuation. As for VEGF and SEMA3F, clusters of tumour cells isolated in the stroma were strongly stained (Figure 1N, P, Q, R). In neuroendocrine tumours (TC, AC, LCNEC, SCLC), NP1 and NP2 levels were significantly lower than in SCC and ADC ($p = 0.0001$ and $p = 0.0031$) and also more heterogeneous, the lowest NP1 scores being observed in SCLC. As for non-neuroendocrine tumours, NP1 and NP2 staining was mainly cytoplasmic with membrane accentuation in LCNEC and carcinoid tumours, whereas SCLC exhibited predominantly cytoplasmic staining.

Statistical correlation between expressions of VEGF, SEMA3F and their receptors NP1 and NP2 in lung tumours

High levels of NP1 and NP2 expression correlated with high levels of VEGF ($p = 0.0043$ and $p = 0.0008$) when all histological types of tumours were considered, to a lesser extent in non-small cell lung carcinoma ($p = 0.03$ for NP1 and $p = 0.01$ for NP2), but not in neuroendocrine tumours, where NP1 and NP2 expression was rather low. The low levels of SEMA3F, VEGF, and NP1–NP2 expression in high-grade NE tumours differ from the patterns observed in carcinoid tumours especially with respect to high SEMA3F expression with a membranous pattern. When considering all tumours combined, we were unable to find a significant inverse correlation between VEGF and SEMA3F staining. However, the rank of VEGF levels of expression was significantly higher than that of SEMA3F in SCC, BC, and LCNEC ($p = 0.007$) (Mann–Whitney test). There was no significant correlation between NP1 and NP2 and SEMA3F. However, when the pattern of SEMA3F staining was considered, higher NP1 scores (ie >150) where observed when SEMA3F staining was only cytoplasmic, both when all lung tumours were analysed together ($p = 0.03$), and when only SCC and ADC were considered ($p = 0.003$) (Mann–Whitney test).

Statistical correlation with clinical stage

As previously noted [25], levels of SEMA3F were significantly lower in advanced tumour stages (III and IV) than in limited stages (I–II) either in non-small cell lung carcinomas (SCC, BC and ADC) ($p = 0.0012$) (Mann–Whitney test) or when all tumours were considered together ($p = 0.0001$). In contrast, neither VEGF, NP1, nor NP2 scores correlated with stage of disease.

Neuropilin subcellular distribution analysed by confocal microscopy in normal and tumour cell lines

Immunostaining of NHBE cells showed a predominantly membrane pattern of NP1 (Figure 2A), consistent with its role as a transmembrane receptor. This pattern of staining was also observed in various lung-derived cell lines, like BEAS2B (SV40-immortalized bronchial epithelium) (Figure 2B) and cervical adenocarcinoma-derived HeLa cells (Figure 2G, J). The membrane staining of NP1 was often brighter at intercellular contacts (Figure 2A, B, G, arrowheads), which suggests an association with cell–cell adhesion structures. Faint granular cytoplasmic staining was also associated with the predominant membrane pattern of NP1. In lung cancer NCI-H661 cells, NP1 and NP2 immunostaining could barely be distinguished from the fluorescent background signal consistent with no specific signal in both cases (Figures 2C, D). The endothelial HUVEC cell line displayed cytoplasmic and membrane staining for both NP1 and NP2 receptors (Figure 2E, F), consistent with paracrine regulation of angiogenesis by secreted VEGF and semaphorins.

Further examination of the subcellular distribution of NP1 in HeLa cells revealed translocation from plasma membrane to cytoplasm depending on cell activity. HeLa cells grown at low density exhibited a majority of interconnected cells with membrane NP1 localization (Figure 2G). However, the cytoplasmic projections in some isolated cells with lamellipodia projections were brightly stained by NP1 antibodies (Figure 2G, arrows). This suggests translocation of NP1 receptors associated with cell migration. Moreover, migrating cells with intense staining of NP1 at the leading edge of lamellipodia also exhibited high SEMA3F staining [25]. In accordance with these observations, HeLa cells with predominantly cytoplasmic distribution of NP1 were rarely observed among confluent cells (Figure 2H), while the occurrence of the cytoplasmic pattern increased from 33% to 51% from the border of a wound through the confluent cell layer (Figure 2J). Since cells at the wound border are apparently stimulated for migration, upregulation of NP1 or translocation to the cytoplasm may be associated with cell invasiveness. Interestingly, some cells located at the border of the wound also displayed brighter staining for SEMA3F (not shown) polarized in the direction of cell migration. Thus, transient upregulation of cytoplasmic SEMA3F may be involved in the control of cell motility with loss of this control occurring in cells from high-grade tumours which exhibit downregulation of SEMA3F expression. On the contrary, NP1 cytoplasmic receptors that are abundantly expressed in high-grade tumours might be implicated in the invasiveness induced by VEGF signalling.

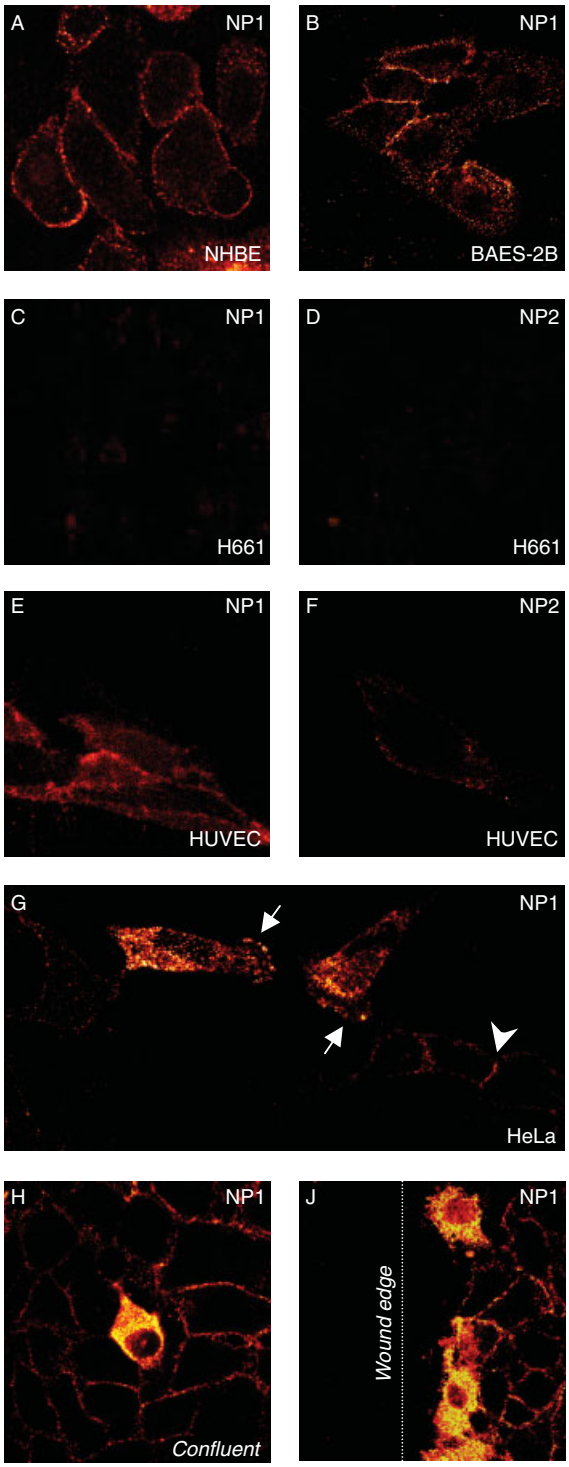

Figure 2. NP1 and NP2 subcellular distribution in normal human bronchial epithelial (NHBE) cells, immortalized epithelial (BAES2B) cells, and the lung tumour cell line NCI- H661, compared with endothelial HUVEC and HeLa cell lines analysed by confocal microscopy (RRX immunostaining). NP1 immunochemistry was performed for NHBE (A), BAES2B (B), NCI-H661 (C), and HUVEC (E) cell lines, HeLa (G–J). NP2 immunochemistry was performed in NCI-H661 (D), HUVEC (F) cell lines. NP1 was present in the cytoplasm of isolated motile cells and at the leading edge of lamellapodia (G, arrows). In non-motile cells, the plasma membrane staining of NP1 was often brighter at intercellular contacts (G, arrowheads). In confluent cells, most NP1 was located at the membrane and only a few cells were labelled in the cytoplasm (H). On the contrary, cells at the border of a wound (dotted line) were positive for NP1 in the cytoplasm (J)

mRNA expression of VEGF, SEMA3F, NP1, and NP2 in lung tumours and cell lines compared with protein expression (Table 3)

In order to assess the presence and level of transcripts and their relationship to protein expression, we compared, in 11 lung tumours and two cell lines, the presence of VEGF, SEMA3F, NP1 and NP2 mRNA with the levels of protein expression observed with all the antibodies used. In NHBE, the high mRNA levels of expression of VEGF and SEMA3F were consistent with the high protein expression observed by immunohistochemistry in normal bronchi (Figure 1A, C), while NP1 and NP2 mRNA were lower. Conversely, the NCI-H661 cell line, which was considered to be negative for NP1 and NP2 expression on the basis of immunocytochemistry, failed to demonstrate the corresponding mRNA, while VEGF and SEMA3F mRNA levels were observed to be low. In lung tumours, SEMA3F, VEGF, NP1 and NP2 mRNA levels showed variations. In tumour 11, the absence of NP1 mRNA and very low NP2 mRNA correlated with the lack of NP1 protein and very low NP2 protein expression as shown by immunohistochemical staining. In contrast, in three lung tumours (tumours 2, 4, 5), we did not observe any staining with both NP1 antibodies despite the presence of NP1 mRNA, suggesting either low antibody sensitivity or absence of protein synthesis. No case revealed positive staining in the absence of mRNA for any protein studied.

Table 3 also includes a comparison of the staining scores observed with the commercially available NP1 and NP2 antibodies (Santa Cruz Biotechnology, Santa Cruz, USA) with those observed with antibodies against NP1 and NP2 provided by Dr A. L. Kolodkin in the same series. In 9 out of 11 and in 8 out of 11 cases respectively, a score variation of less than 30/300 was observed, allowing a concordance of 82% and 73% for the NP1 and NP2 antibodies from both sources respectively. This high concordance illustrated in 11 lung tumours is in agreement with that observed with 104 tissues from our series (see Material and methods), validating the use of both the commercially available NP1 and NP2 antibodies and those from A. L. Kolodkin.

Discussion

VEGF expression, and in some instances expression of the VEGF receptors Flk-1 and Flt-1, has been reported in a variety of premalignant lesions, invasive tumours, and cell lines, including cervical intraepithelial neoplasia, colonic carcinoma, glioma, breast carcinoma, gastric carcinoma, melanoma, head and neck cancer, lung cancer [18,19,34,35], as well as in squamous dysplastic cells [35]. In the present study, we identified a significant increase in VEGF expression in most of the preneoplastic bronchial lesions ranging from moderate to severe dysplasia and *in situ* carcinoma,

Table 3. Analysis of 11 lung tumours and two cell lines for VEGF, SEMA3F, NP1, and NP2 expression by real-time quantitative RT-PCR and comparison with corresponding staining scores for protein expression obtained by immunohistochemistry

Tumours: histological type	VEGF mRNA	VEGF scores	SEMA3F mRNA	SEMA3F scores	NP1 mRNA	NP1 scores K	NP1 scores SC	NP2 mRNA	NP2 scores K	NP2 scores SC
Tumour 1: ADC	53.66	100	58.72	50	13.6	160	160	3.96	160	160
Tumour 2: SCC	13.6	240	58.72	0	9.16	0	0	0.79	30	0
Tumour 3: SCC	8.37	0	13.32	240	3.15	160	60	1.47	60	50
Tumour 4: ADC	45.44	20	23.04	300	7.39	0	0	2.12	160	80
Tumour 5: ADC	60.37	30	52.56	20	12.96	0	0	8.85	60	50
Tumour 6: ADC	16.63	60	7.87	100	5.01	0	20	4.19	50	50
Tumour 7: ADC	360.98	160	61.64	160	35.16	80	80	7.7	160	100
Tumour 8: SCC	45.44	100	67.92	30	1.6	0	30	10.82	80	50
Tumour 9: SCC	12.69	100	96.72	160	3.85	0	100	4.04	50	100
Tumour 10: SCC	16.06	120	35.16	160	1.39	60	60	1.98	120	60
Tumour 11: SCC	17.82	100	25.03	30	0.062	0	10	0.87	60	60
Cell lines										
NHBE	27.2		31.25		2.76			7.55		
NCI-H661	9.29		4.74		0.01			0.32		

Results expressed in terms of relative expression (×1000) compared with G3PDH.
K for antibodies provided by A. L. Kolodkin, SC for commercial antibodies.
SCC, squamous cell carcinoma; ADC, adenocarcinoma.

with a rather constant level of expression in corresponding microinvasive and invasive cancers. This is in agreement with a previous report demonstrating strong VEGF expression in high-grade laryngeal dysplasia [36]. However, there have been other reports of bronchial or head and neck premalignant lesions where no statistical difference in VEGF expression was observed despite significant increases in microvascular density [11]. These discrepancies may be technical in nature or suggest that VEGF entails other functions than angiogenesis in tumours such as an autocrine loop on tumour cells themselves, migration or survival. We failed to detect any differences in VEGF expression between angiogenic squamous dysplasia and other classical dysplasia, suggesting that this morphological variant has causes other than elevated VEGF expression *per se*. Consistent with this assumption angiogenic squamous dysplasia is exclusively encountered in cigarette smokers, and stimulation of angiogenesis and tumour growth by nicotine has been recently demonstrated in a mouse model [37]. Alternatively, it is becoming increasingly clear that VEGF has independent effects on tumour cells, possibly acting through VEGF receptors and/or NP receptors, such as the autocrine survival activity reported by Bachelder *et al* in breast cancer cells [38]. A functional VEGF/VEGFR2 autocrine loop was demonstrated in gastric tumour cell lines [19]. Similarly, in melanoma VEGF was shown to have positive effects on migration acting through an integrin-dependent pathway involving phosphatidylinositol-3-kinase [39]. Interestingly, VEGF was shown to stimulate cellular invasion of breast cancer cells, signalling through the same PI3 kinase pathway despite low levels of Flt-1 and KDR mRNA [40]. Thus, it is not surprising that elevated levels of VEGF can be observed in premalignant lesions independently of neoangiogenesis.

As previously reported in lung cancers [11,18,25], VEGF is widely expressed in SCC and ADC, with cytoplasmic staining associated with strong membrane staining. In microinvasive and invasive SCC, tumour cells either at the periphery of lobules or isolated in the stroma were strongly VEGF positive, consistent with a role for VEGF in cell migration. We failed to observe any correlation between VEGF overexpression and advanced stages of the disease, in keeping with our previous results [18]. In contrast with non-small cell carcinomas, we observed that VEGF was weakly expressed in neuroendocrine tumours, particularly in SCLC. Interestingly, c-myc overexpression, which is frequent in SCLCs, has been reported to downregulate VEGF transcription [41].

In contrast to VEGF, SEMA3F expression was lost early in preinvasive lesions and corresponding tumours. This is consistent with reports that 3p21.3 loss of heterozygosity is both frequent and appears to be the earliest 3p event in lung cancer development [42]. Expression of the second allele might also be impaired. Because loss of SEMA3F staining occurred in most premalignant lesions, we did not observe differences between dysplasia of any type and *in situ* or invasive carcinoma. As was expected based on our previous studies, low levels of SEMA3F expression were observed in lung tumours with reduced or absent membrane staining and cytoplasmic delocalization, except in carcinoid tumours and well-differentiated adenocarcinomas. Interestingly, in these tumours VEGF scores were lower than SEMA3F, which is a unique situation among lung tumours. Thus, the preservation of SEMA3F membrane staining may depend on VEGF expression with competition for NP binding at the cell surface, as well as being affected by 3p LOH.

Although we did not observe any correlation between VEGF overexpression and advanced stages of disease, we confirmed a strong correlation between

loss of membrane to cytoplasmic delocalization of SEMA3F and advanced stage, suggesting that SEMA3F functions are impaired in lung cancer. In support of this, another gene involved in the semaphorin pathway, collapsin response mediator protein-1 (CRMP-1), has been recently shown to correlate inversely with the invasive capability of lung cancer cell lines [43]. Thus, there is growing evidence from independent sources indicating that the loss of semaphorin signalling is important in lung cancer development.

Upregulation of NP1 has been implicated in tumour progression as it has been correlated with advanced stages in prostatic tumours and malignant behaviour in astrocytomas [44,45]. In breast cancer cell lines, VEGF has been reported to act as an autocrine survival factor [38] and in gastric adenocarcinoma cells as an autocrine factor for proliferation [19]. Interestingly, a NP1 blocking antibody eliminated this function in the absence of demonstrable Flk-1/KDR expression [38] and NP1 expression has been described in various tumour cell lines with or without concomitant KDR [16,19]. Our wound assay suggests that NP1 functions in cell migration as has already been demonstrated *in vitro* in rat prostate carcinoma [17]. However, whether NP1 cytoplasmic delocalization and increase of its expression are consistent with the activation of an NP1-dependent pathway leading to increased endocytosis cannot be assessed from the present results. Nevertheless, it would be consistent with our finding of NP1/NP2 overexpression in tumour cells migrating away from the tumour bulk. Like NP1, NP2 overexpression was reported in osteosarcomas and melanoma in association with VEGF expression, angiogenesis, and tumour growth [21,22]. In preinvasive bronchial lesions, we demonstrated a strong increase of NP1 and NP2 with more aggressive histological grades of dysplasia and *in situ* carcinoma. As perhaps anticipated, lung tumours expressing high VEGF levels also overexpressed NP1 and NP2 with a statistical direct correlation. Selective induction of NP1 by VEGF and membrane translocation has been demonstrated in bovine endothelial cells at the level of mRNA and protein synthesis [46]. NP2 could well be stimulated also by VEGF in endothelial cells via VEGFR2 [19]. In contrast to what was observed in SCC and ADC, the VEGF/SEMA3F/NP pathway appears to be characterized by the preservation of SEMA3F expression in carcinoid tumours. Conversely SCLC, a high-grade neuroendocrine tumour, exhibited much lower levels of VEGF and NP expression concomitant with the loss or marked reduction of SEMA3F in most cases. We also observed, in tumours, individual tumour cells or tumour cell clusters which stained strongly for VEGF, SEMA3F and neuropilins. Whether low-grade preinvasive lesions containing clusters of VEGF-positive cells signify a worse prognosis is currently unknown but deserves further study. While VEGF expression in addition to neuropilins might be dynamic in low-grade lesions, VEGF might be involved in selection of clones during tumour progression as most high-grade preinvasive lesions were positive. On the other hand, SEMA3F overexpression may inhibit cell migration and may function as an anti-survival factor. In favour of this, we have shown that SEMA3F overexpression induces apoptosis in mammary adenocarcinoma cells (Nasarre *et al*, personal communication) and in the large-cell NSCLC cell line, NCI H661 (data not shown). Similar results have been obtained for SEMA3B in lung carcinoma cell lines [47]. Furthermore a recent study indicates that SEMA3F suppresses tumour formation in inducible clones *in vitro* and *in vivo* in nude mice and reduces apoptosis. Interestingly a SCLC cell line was resistant to SEMA3F-induced tumour suppression [48]. However, the consequence of high SEMA3F expression in addition to VEGF in some cell clusters is hard to predict as a balance between SEMA3A and VEGF modulates not only apoptotic process but also cellular motility [32]. One hypothesis is that VEGF might protect against death induced by SEMA3F upregulation in migrating cells.

In summary, the VEGF/SEMA3F/NP pathway appears to be commonly deregulated in lung cancer pathogenesis. Loss of SEMA3F surface staining is an early event and the degree of loss correlates with tumour stage. VEGF staining increases progressively with worsening dysplasia and focal areas of individual cells or clusters staining positively for VEGF can be detected even in low-grade dysplasias. Increased NP staining occurs in conjunction with increased VEGF. Based on our current understanding of this system, we would anticipate that semaphorin replacement combined with anti-VEGF approaches should be additive or even synergistic in the treatment of established tumours, as previously inferred [48]. Because alterations in VEGF/SEMA3F/NP pathway occur early, targeted therapies should also be advantageous for premalignant lesions.

Acknowledgements

We are very grateful to Dr Kolodkin for providing us with the neuropilin antibodies. We thank Anne Cantereau for technical assistance in the confocal microscopy studies performed in the confocal microscopy core of the Research Federative Institute IFR59 at the University of Poitiers. The following sponsors are acknowledged: INSERM, Ligue Nationale contre le Cancer, and ARC (S. L. and E. B.), CNRS, ARC, and Ligue contre le Cancer (Comité de la Vienne et de la Charente) (J. R.), University of Colorado Lung Cancer SPORE CA5187-07 (H. D).

References

1. Souhami R. Lung cancer. *Br Med J* 1992; **304**: 1298–1301.
2. Gazdar A. The molecular and cellular basis of human lung cancer. *Anticancer Res* 1994; **13**: 561–568.
3. Travis WD, Colby TV, Corrin B, Shimosato Y, Brambilla E, in collaboration with Sobin LH and pathologists from 14 countries. *International Histological Classification of Tumors: World Health Organization* (3rd edn). Springer: Berlin, 1999.

4. Vogelstein B, Kinzler KW. The multistep nature of cancer. *Trends Genet* 1993; **9**: 138–141.
5. Auerbach O, Hammond EC, Garfinkel I. Changes in bronchial epithelium in relation to cigarette smoking 1955–1060 vs 1970–1977. *N Engl J Med* 1979; **300**: 381–386.
6. Brambilla E, Gazzeri S, Lantuejoul S, *et al*. p53 mutant immunophenotype and deregulation of p53 transcription pathway (Bcl2, Bax, and Waf1) in precursor bronchial lesions of lung cancer. *Clin Cancer Res* 1998; **4**: 1609–1618.
7. Lonardo F, Rush V, Langenfeld J, Dmitrovsky E, Klimstra DS. Overexpression of cyclins D1 and E is frequent in bronchial preneoplasia and precedes squamous cell carcinoma development. *Cancer Res* 1999; **15**: 2470–2476.
8. Brambilla E, Gazzeri S, Moro D, Lantuejoul S, Veyrenc S, Brambilla C. Alterations of Rb pathway (Rb-p16INK4-cyclin D1) in preinvasive bronchial lesions. *Clin Cancer Res* 1999; **5**: 243–250.
9. Siemeister G, Martigny-Baron G, Marme D. The pivotal role of VEGF in tumor angiogenesis: molecular facts and therapeutic opportunities. *Cancer Metastasis* 1998; **17**: 241–248.
10. Kim KJ, Li B, Winer J, *et al*. Inhibition of vascular endothelial growth factor-induced angiogenesis suppresses tumour growth in vivo. *Nature* 1993; **362**: 841–844.
11. Fontanini G, Calcinai A, Boldrini L, *et al*. Modulation of neoangiogenesis in bronchial preneoplastic lesions. *Oncol Rep* 1999; **6**: 813–817.
12. Keith RL, Miller YE, Gemmill RM, *et al*. Angiogenic squamous dysplasia in bronchi of individuals at high risk for lung cancer. *Clin Cancer Res* 2000; **6**: 1616–1625.
13. Kolodkin AL, Levengood D, Rowe E, Tai Y, Giger R, Ginty D. Neuropilin is a semaphorin III receptor. *Cell* 1997; **90**: 753–762.
14. He Z, Tessier-Lavigne M. Neuropilin is a receptor for the axonal chemorepellent semaphorin III. *Cell* 1997; **90**: 739–751.
15. Unified nomenclature for the semaphorins/collapsins: Semaphorin Nomenclature Committee. *Cell* 1999; **97**: 551–552.
16. Soker S, Takashima S, Miao HQ, Neufeld G, Klagsbrun M. Neuropilin-1 is expressed by endothelial and tumor cells as an isoform-specific receptor for vascular endothelial growth factor. *Cell* 1998; **92**: 735–745.
17. Miao HQ, Lee P, Lin H, Soker S, Klagsbrun M. Neuropilin-1 expression by tumor cells promotes tumor angiogenesis and progression. *FASEB J* 2000; **14**: 2532–2539.
18. Decaussin M, Sartelet H, Robert C, *et al*. Expression of vascular endothelial growth factor (VEGF) and its two receptors (VEGF-R1-Flt1 and VEGF-R2-Flk1/KDR) in non small cell lung carcinomas (NSCLCs): correlation with angiogenesis and survival. *J Pathol* 1999; **188**: 369–377.
19. Tian X, Song S, Wu J, Meng L, Dong Z, Shou C. Vascular endothelial growth factor: acting as an autocrine growth factor for human gastric adenocarcinoma cell MGC803. *Biochem Biophys Res Commun* 2001; **286**: 505–512.
20. Chen H, Chedotal A, He Z, Goodman CS, Tessier-Lavigne M. Neuropilin-2, a novel member of the neuropilin family, is a high affinity receptor for the semaphorins SemaE and SemaIV but not SemaIII. *Neuron* 1997; **19**: 547–559.
21. Handa A, Tokunaga T, Tsuchida T, *et al*. Neuropilin-2 expression affects the increased vascularization and is a prognostic factor in osteosarcoma. *Int J Oncol* 2000; **17**: 291–295.
22. Lacal PM, Faila CM, Pagani E, *et al*. Human melanoma cells secrete and respond to placenta growth factor and vascular endothelial growth factor. *J Invest Dermatol* 2000; **115**: 1000–1007.
23. Kagoshima M, Ito T, Kitamura H, Goshima Y. Diverse gene expression and function of semaphorins in developing lung: positive and negative regulatory roles of semaphorins in lung branching and morphogenesis. *Genes Cells* 2001; **6**: 559–571.
24. Christensen CR, Klingelhofer J, Tarabykina S, Hulgaard EF, Kramerov D, Lukanidin E. Transcription of a novel mouse semaphorin gene, M-semaH, correlates with the metastatic ability of mouse tumor cell lines. *Cancer Res* 1998; **58**: 1238–1244.
25. Brambilla E, Constantin B, Drabkin H, Roche J. Semaphorin SEMA3F localization in malignant human lung and cell lines: a suggested role in cell adhesion and migration. *Am J Pathol* 2000; **156**: 939–950.
26. Sekido Y, Bader S, Latif F, *et al*. Human semaphorins A (V) and (IV) reside in the 3p21.3 small cell lung cancer deletion region and demonstrate distinct expression patterns. *Proc Natl Acad Sci USA* 1996; **93**: 4120–4125.
27. Roche J, Boldog F, Robinson M, *et al*. Distinct 3p21.3 deletions in lung cancer and identification of a new human semaphorin. *Oncogene* 1996; **12**: 1289–1297.
28. Chen H, He Z, Bagri A, Tessier-Lavigne M. Semaphorin–neuropilin interactions underlying sympathetic axon to class III semaphorins. *Neuron* 1998; **21**: 1283–1290.
29. Takahashi T, Fournier A, Nakamura F, *et al*. Plexin–neuropilin-1 complexes from functional semaphorin-3A receptors. *Cell* 1999; **99**: 59–69.
30. Miao HQ, Soker S, Feiner L, Alonso JL, Raper JA, Klagsbrun M. Neuropilin-1 mediates collapsin-1/semaphorin III inhibition of endothelial cell motility: functional competition of collapsin-1 and vascular endothelial growth factor-165. *J Cell Biol* 1999; **146**: 233–242.
31. Giger RJ, Urquart ER, Gillespie SKH, Levengood DV, Ginty DD, Kolodkin AL. Neuropilin-2 is a receptor for semaphorin IV: insight into the structural basis of receptor function and specificity. *Neuron* 1998; **21**: 1079–1092.
32. Bagnard D, Vaillant C, Khuth ST, *et al*. Semaphorin 3A-vascular endothelial growth factor-165 balance mediates migration and apoptosis of neural progenitor cells by the recruitment of shared receptor. *J Neurosci* 2001; **21**: 3332–3341.
33. Hirsch E, Hu L-J, Prigent A, *et al*. Distribution of semaphorin IV in adult human brain. *Brain Res* 1999; **823**: 67–79.
34. Dobbs SP, Hewette PW, Johnson IR, Carmichael J, Murray JC. Angiogenesis is associated with vascular endothelial growth factor expression in cervical intraepithelial neoplasia. *Br J Cancer* 1997; **76**: 1410–1415.
35. Herold-Mende C, Steiner HH, Andl T, *et al*. Expression and functional significance of vascular endothelial growth factor receptors in human tumor cells. *Lab Invest* 1999; **79**: 1573.
36. Denhart BC, Guidi AJ, Tognazzi K, Dvorak HF, Brown LF. Vascular permeability factor/vascular endothelial growth factor and its receptors in oral and laryngeal squamous cell carcinoma and dysplasia. *Lab Invest* 1997; **6**: 659–664.
37. Heeschen C, Jang JJ, Weis M, *et al*. Nicotine stimulates angiogenesis and promotes tumor growth and atherosclerosis. *Nat Med* 2001; **7**: 833–839.
38. Bachelder R, Crago A, Chung J, *et al*. Vascular endothelial growth factor is an autocrine survival factor for neuropilin-expressing breast carcinoma cells. *Cancer Res* 2001; **61**: 5736–5740.
39. Byzova TV, Goldman CK, Pampori N, *et al*. A mechanism for modulation of cellular responses to VEGF: activation of the integrins. *Mol Cell* 2000; **6**: 851–860.
40. Price DJ, Miralem T, Jiang S, Steinberg R, Avraham H. Role of vascular endothelial growth factor in the stimulation of cellular invasion and signaling of breast cancer cells. *Cell Growth Diff* 2001; **12**: 129–135.
41. Barr LF, Campbell SE, Diette GB, *et al*. C-Myc suppresses the tumorigenicity of lung cancer cells and down regulates vascular endothelial growth factor expression. *Cancer Res* 2000; **60**: 143–149.
42. Wistuba II, Behrens C, Virmani AK, *et al*. High resolution chromosome 3p allelotyping of human cancer and preneoplastic/preinvasive bronchial epithelium reveals multiple, discontinuous sites of 3p allele loss and three regions of frequent breakpoints. *Cancer Res* 2000; **60**: 1949–1960.
43. Shi JY, Yang SC, Hong TM, *et al*. Collapsin response mediator protein-1 and the invasion and metastasis of cancer cells. *J Natl Cancer Inst* 2001; **93**: 1392–1400.
44. Latil A, Bieche I, Pesche S, *et al*. VEGF overexpression in clinically localized prostate tumors and neuropilin-1 overexpression in metastatic forms. *Int J Cancer* 2000; **89**: 167–172.
45. Ding H, Wu X, Roncari L, *et al*. Expression and regulation of neuropilin-1 in human astrocytomas. *Int J Cancer* 2000; **88**: 584–592.

46. Oh H, Takagi H, Otani A, *et al*. Selective induction of neuropilin-1 by vascular endothelial growth factor (VEGF): a mechanism contributing to VEGF- induced angiogenesis. *Proc Natl Acad Sci USA* 2002; **99**: 383–388.
47. Tomizawa Y, Sekido Y, Kondo M, *et al*. Inhibition of lung cancer cell growth and induction of apoptosis following re-expression of 3p21.1 candidate tumor suppressor gene SEMA3B. *Proc Natl Acad Sci USA* 2001; **98**: 13954–13959.
48. Xiang R, Davalos AR, Hensel CH, Zhou XJ, Tse C, Naylor SL. Semaphorin 3F gene from human 3p21.3 suppresses tumor formation in nude mice. *Cancer Res* 2002; **62**: 2637–2643.

